Düzce University
Journal of Science & Technology

Research Article

Investigation on the Effect of Parasitic Elements on PID Control of DC-DC Buck Converter

Mustafa İNCİ[a,*], Yusuf ALTUN[b]

[a]*Volta Motor Industry and Trade Inc. Design Center, Cumayeri Factory, Düzce/Türkiye.*
[b]*Düzce University, Engineering Faculty, Department of Computer Engineering, Düzce/Türkiye.*
** Corresponding author's e-mail address: yusufaltun@duzce.edu.tr*
DOI: 10.29130/dubited.1454306

ABSTRACT

DC-DC converter circuits are used in many electronic devices to adjust the voltage to a certain level such as Electric Vehicle. DC-DC Buck converters, which are the most used type of DC-DC converters, reduce the input voltage and keep the output voltage constant at a desired reference voltage value. In this study, the effect of parasitic elements in Buck DC-DC converters is examined on the PID controllers. Parasitic elements cause a non-linear effect on the Buck converter system model. Studies in the literature generally control the output voltage by designing controllers on the Buck converter model without parasitic elements. Alternatively, linear controllers such as PID are designed according to the linearizing model, taking into account the effect of parasitic elements. In addition, nonlinear controllers are designed on the full model with the effect of parasitic elements. In this study, the effect of parasitic elements on linear controllers, especially PID, is examined.

Keywords: *DC-DC converter, Buck converter, Parasitic elements, PID controller*

Parazitik Elemanların DC-DC Buck Dönüştürücünün PID Kontrolüne Etkisinin İncelenmesi

ÖZ

DC-DC dönüştürücü devreleri Elektrikli Araçlar gibi birçok elektronik cihazda gerilimi belirli düzeye ayarlamak için kullanılmaktadır. DC-DC dönüştürücülerin yaygın kullanılan türü olan Buck DC-DC dönüştürücüler giriş gerilimini düşürerek çıkış gerilimini istenen bir referans gerilim değerinde sabit tutar. Bu çalışmada, Buck DC-DC dönüştürücülerdeki parazitik elemanların PID kontrolcüler üzerindeki etkisi incelenmiştir. Parazitik elemanlar Buck dönüştürücü sistem modeli üzerinde lineer olmayan etkiye neden olmaktadır. Literatürde yapılan çalışmalar genellikle parazitik elemanlar olmaksızın Buck dönüştürücü modeli üzerinde kontrolcüler tasarlanarak çıkış gerilimi kontrol edilmektedir. Alternatif olarak, parazitik elemanların etkisi de dikkate alınan model doğrusallaştırılarak lineer kontrolcüler tasarlanmaktadır. Bunlara ek olarak, parazitik elemanların etkisiyle birlikte tam model üzerinde lineer olmayan kontrolcüler tasarlanmaktadır. Bu çalışmada ise parazitik elemanların özellikle PID gibi lineer kontrolcü üzerindeki etkisi incelenmiştir.

Anahtar Kelimeler: *DC-DC dönüştürücü, Buck dönüştürücü, Parazit elemanlar, PID kontrolör*

Received: 17/03/2024, Revised: 02/04/2024, Accepted: 02/04/2024

I. INTRODUCTION

DC-DC converters are widely used in electronic devices to regulate DC voltage. They are capable of converting voltage from one level to another. Their objective is to regulate and manage the transfer of electrical energy between input and output by adjusting voltages and currents to be compatible with loads. Switches, diodes, inductors, and capacitors play crucial roles as energy storage elements within converter circuits. Modern DC-DC converters are advanced power electronic devices that utilize high-frequency switching circuits with pulse width modulation (PWM) technique. These converters are utilized for numerous applications in industry and academia [1], [2], [3], [4], [5], [6], [7], [8], [9]. The extraordinary increase in their benefits is particularly obvious in sustainable energy systems such as wind turbines, photovoltaics, AC transmission and battery storage [10]. The growth of DC microgrids [4], [9], [11] is encouraging larger applications of DC-DC converters in next power systems. DC microgrids are becoming increasingly popular and a more suitable alternative to AC microgrids due to their simpler power converter stages, flexible control algorithms etc. However, DC microgrids can face instability issues due to non-linear loads like constant power loads (CPL), which have a higher negative impedance, leading to potential voltage collapse on the primary DC Bus. DC voltages produced by fuel cells, batteries or photovoltaic systems change in amplitude; input voltages of power-factor adjustment applications change with sinusoidal grid voltages; and large-scale reconfiguration of battery packs causes voltage spikes [12], [13], [14]. Therefore, good control design requires adjusting the output voltage. DC-DC converters play a crucial role in Electric Vehicles, which are extensively utilized today, leading to ongoing research on different circuits and controls, as evidenced in the studies mentioned in [1], [15], [16], [17].

One type of commonly used of DC-DC converters are Buck (step down) converter. Buck converters utilize a straightforward yet highly efficient circuit configuration to reduce the input voltage to a lower output level. They are electronic circuits that play a significant role in electrical power systems and have a wide range of applications. Their application areas are in the various electronic devices such as cell phones, televisions, and computers. Also, they are widely used in solar energy systems, where they convert high-voltage DC power from solar panels to lower voltage levels suitable for use and integration with the electrical grid or battery banks such as DC microgrids [18], [19], [20], photovoltaic systems/solar panels [21], [22]. In addition, it is used for DC motor control such as [23], [24], [25]. Additionally, they are frequently found in the power systems of electric vehicle and hybrid vehicle, where they are employed to meet the power demands of onboard electronic systems and lighting by reducing the voltage from the battery [25], [26], [27], [28], [29]. Moreover, in the telecommunications industry, DC-DC Buck converters are often utilized to enhance energy efficiency and optimize power distribution [30]. Finally, they play a crucial role in power conversion and control in industrial equipment and automation systems. DC-DC Buck converters are regarded as essential components in various applications, contributing to energy efficiency, voltage regulation, and effective power distribution in modern electronic systems. Finally, they contribute significantly to power conversion and control, facilitating the efficient operation of many industrial systems.

The presence of parasitic elements, such as resistance, in DC-DC buck converters can have significant effects on their performance. These parasitic elements, often inherent in real-world components, can lead to power loss, reduced efficiency, and decreased voltage regulation. Studies have shown that even small amounts of resistance, particularly in high-power applications, can significantly sap the converter's ability to deliver power efficiently. Additionally, they can cause instability in the converter's dynamic response, impacting its ability to quickly adjust to changes in load or input voltage. Researchers have investigated methods to mitigate these effects, including careful component selection, layout optimization, and advanced control techniques. By addressing parasitic elements, engineers can improve the overall performance and reliability of DC-DC buck converters such as in [31], [32], [33], [34]. For example, in [35], the effect of parasitic resistances on the input resistance in Maximum Power Point Tracking (MPPT) systems of photovoltaic (PV) systems has been investigated. [31] introduces a new method utilizing Adaptive Backstepping for developing a current controller in buck-boost converters by including influence of parasitic elements. [36] discusses the fixed diode duty

cycle operation of Buck converter, considering the parasitic resistances. A simple circuit-level model is presented to explain how undesirable trigger signals occur at the input voltage of a MOSFET in a synchronous converter. [37]. It considers the parasitic inductances and capacitances of both the control and the synchronous MOSFETs, as well as the reverse recovery properties of the synchronous MOSFET's body diode. In [32], a new approach is proposed for the passivity-based nonlinear control design of the buck converter, where the design considers the full converter model, including the impacts of parasitic elements such as equivalent series resistance (ESR) of inductor, ESR of MOSFET. In [38], a nonlinear way/model is proposed to model Buck an Boost converters for both without parasitic elements and with parasitic elements. In [39], the effect of parasitic elements on the output voltages has been investigated. In [40], the effects of parasitic elements have been investigated on power loss in buck converter-based GaN. Finally, parasitic elements can significantly impact the performance of DC-DC buck converters. By understanding their effects and employing proper design techniques, such as minimizing parasitic resistance and inductance, optimizing layout, and selecting appropriate components, converter efficiency, stability, and transient response can be improved.

The aforementioned-works and other relevant studies in the literature are generally related to the effects of parasitic elements on the circuits. However, their effects on control design are not comprehensively examined. This paper presents a comprehensive analysis of control performance and control design challenges caused by parasitic elements in DC-DC Buck converters. As seen in [34], the Buck converter system becomes nonlinear although the values of parasitic elements are low. Therefore, the major problem is that parasitic elements cause nonlinearity due to switching duty ratio. Different controller or different modelling have been proposed to overcome the difficulties. For example, to develop the controller response, the inductor parasitic resistance is modelled for Boost converter in [41]. Additionally, a PID controller is employed to remove any steady-state error of the system. An adaptive nonlinear controller is developed for a DC-DC buck/boost converter, ensuring robustness and stability even with changes in converter load, fluctuations in input voltage, and uncertainties in parameters in [42]. On the other hand, the controller design endures the linearized model of the converter as in [43], where employing this method across a broad spectrum of input voltage fluctuations, load resistances, and desired voltage variations may lead to instability in the converter. Similarly, [44] use the linearized DC-DC boost converter model. Alternatively, nonlinear controllers such as model feedback linearisation, sliding mode, predictive control, fuzzy control are designed for the nonlinear converter model with parasitic elements such as [31], [33], [41], [45], [46], [47]. Therefore, the nonlinear controller design is usually needed if the model is not linearized. However, linear control such as PID is simpler and cheaper. Hence, it depends on linearizing the converter model with parasitic elements or without parasitic elements. As for the analysis in this paper, the effects of PID controllers on the full model containing parasitic elements are investigated.

II. BUCK CONVERTER MODEL

A. DC-DC BUCK CONVERTER CLASSIC/LINEAR MODEL (WITHOUT PARASITIC ELEMENTS))

Figure 1 shows the circuit model of DC-DC Buck converter without parasitic elements. Let's consider the on-state of the MOSFET. According to the equation $v_o = v_C$, when Kirchhoff's voltage law is applied, Equation (1) is obtained, and when it is rearranged, Equation (2) is obtained.

$$V_{in} = L\frac{di_L}{dt} + v_C \tag{1}$$

$$V_{in} - L\frac{di_L}{dt} - v_C = 0 \tag{2}$$

When Kirchhoff's current law is applied, Equation (3) is obtained, and when it is rearranged, Equation (4) is obtained.

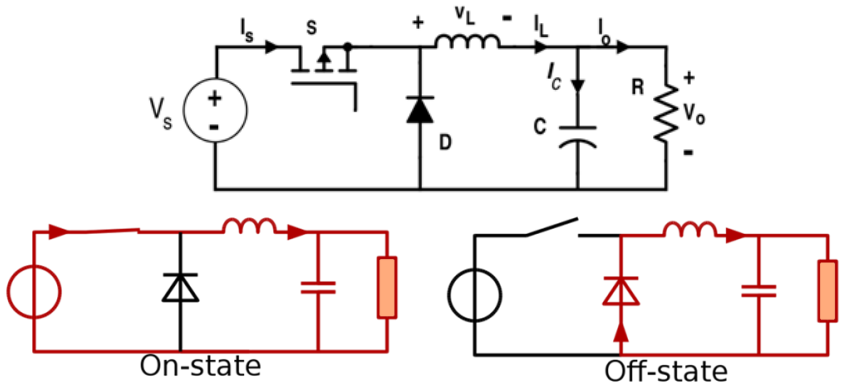

Figure 1. *Buck converter on-off state*

$$i_O + i_C - i_L = 0 \tag{3}$$

$$\frac{v_C}{R} + C\frac{dv_C}{dt} - i_L = 0 \tag{4}$$

When Equation (2) and Equation (4) are rearranged, Equation (5) is obtained.

$$\begin{aligned} \frac{di_L}{dt} &= \frac{1}{L}(V_{in} - v_C) \\ \frac{dv_C}{dt} &= \frac{1}{C}\left(i_L - \frac{v_C}{R}\right) \end{aligned} \tag{5}$$

Using Equation (5) and Equation $v_o = v_C$, the state space matrices in Equation (6) are obtained as in Equation (7).

$$\begin{aligned} \dot{x}(t) &= Ax(t) + Bu(t) \\ y(t) &= Cx(t) + Du(t) \end{aligned} \tag{6}$$

$$\underbrace{\begin{bmatrix} \frac{dI_L}{dt} \\ \frac{dV_C}{dt} \end{bmatrix}}_{\dot{x}} = \underbrace{\begin{bmatrix} 0 & \frac{-1}{L} \\ \frac{1}{c} & \frac{-1}{Rc} \end{bmatrix}}_{A_{on}} \underbrace{\begin{bmatrix} I_L \\ V_C \end{bmatrix}}_{x} + \underbrace{\begin{bmatrix} \frac{1}{L} \\ 0 \end{bmatrix}}_{B_{on}} \underbrace{[V_{in}]}_{u}$$

$$y = \underbrace{[0 \quad 1]}_{C_{on}} \underbrace{\begin{bmatrix} I_L \\ V_C \end{bmatrix}}_{x} \tag{7}$$

Similarly, we get the state space equation in (8).when we consider the off-state of the MOSFET in Figure 1.

$$\underbrace{\begin{bmatrix} \frac{dI_L}{dt} \\ \frac{dV_C}{dt} \end{bmatrix}}_{\dot{x}} = \underbrace{\begin{bmatrix} 0 & \frac{-1}{L} \\ \frac{1}{c} & \frac{-1}{Rc} \end{bmatrix}}_{A_{off}} \underbrace{\begin{bmatrix} I_L \\ V_C \end{bmatrix}}_{x} + \underbrace{\begin{bmatrix} 0 \\ 0 \end{bmatrix}}_{B_{off}} \underbrace{\begin{bmatrix} V_{in} \end{bmatrix}}_{u}$$
$$y = \underbrace{\begin{bmatrix} 0 & 1 \end{bmatrix}}_{C_{off}} \underbrace{\begin{bmatrix} I_L \\ V_C \end{bmatrix}}_{x} \tag{8}$$

Now let's derive the state space average model. Since the duty ratio (d) of the period is in conduction and the (1-d) ratio is in cutoff, the average model is obtained as in Equation (9), where d is MOSFET switching duty ratio ranging between 0 and 1.

$$\begin{aligned} A &= d \times A_{on} + (1-d) \times A_{off} \\ B &= d \times B_{on} + (1-d) \times B_{off} \\ C &= d \times C_{on} + (1-d) \times C_{off} \end{aligned} \tag{9}$$

If we apply the average model approach in Equation (9), we get (10) state space average model.

$$\underbrace{\begin{bmatrix} \frac{dI_L}{dt} \\ \frac{dV_C}{dt} \end{bmatrix}}_{\dot{x}} = \underbrace{\begin{bmatrix} 0 & \frac{-1}{L} \\ \frac{1}{c} & \frac{-1}{cR} \end{bmatrix}}_{A} \underbrace{\begin{bmatrix} I_L \\ V_C \end{bmatrix}}_{x} + \underbrace{\begin{bmatrix} \frac{V_{in}}{L} \\ 0 \end{bmatrix}}_{B} \underbrace{\begin{bmatrix} d \end{bmatrix}}_{u}$$
$$y = \underbrace{\begin{bmatrix} 0 & 1 \end{bmatrix}}_{C} \underbrace{\begin{bmatrix} I_L \\ V_C \end{bmatrix}}_{x} \tag{10}$$

B. DC-DC BUCK CONVERTER FULL MODEL (WITH PARASITIC ELEMENTS)

In electrical circuits, a parasitic element is a circuit element (such as resistance, inductance or capacitance) that is present in an electrical component but occurs outside its intended purpose and is not desired. For example, a resistor may have undesirable parasitic capacitance at high frequencies beyond its specification. Figure 2 shows the converter circuit including parasitic elements (parasitic resistances). r_m, r_D r_L and r_c are the parasitic resistances of the MOSFET, diode, inductor, and capacitor, respectively. In addition, the diode forward voltage is V_D. It is supposed that the forward voltage is zero.

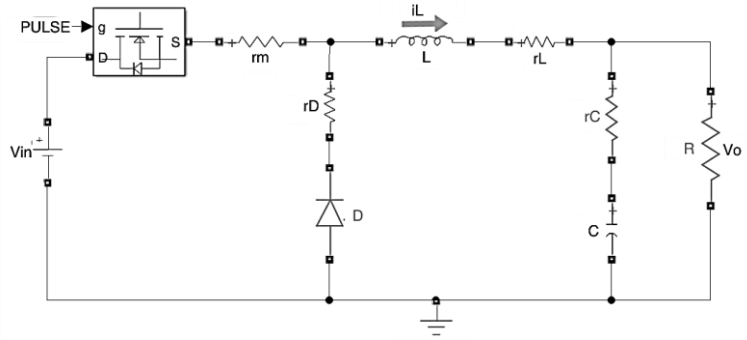

Figure 2. *Buck converter circuit with parasitic resistances*

Similar to the modelling steps in Section A can be applied for this circuit. After the steps, we get state space average model (11). (12) is obtained from full model (11) for $r_m = r_D = 0$. Therefore, the system model is linearized.

$$\begin{bmatrix} \frac{dI_L}{dt} \\ \frac{dV_C}{dt} \end{bmatrix} = \begin{bmatrix} \frac{-1}{L}\left(d\left(r_m - r_D\right) + r_D + r_L + \frac{r_C R}{\left(r_C + R\right)} \right) & \frac{-1}{L}\frac{R}{\left(r_C + R\right)} \\ \frac{1}{c}\frac{R}{\left(r_C + R\right)} & \frac{-1}{c}\frac{1}{\left(r_C + R\right)} \end{bmatrix} \begin{bmatrix} I_L \\ V_C \end{bmatrix} + \begin{bmatrix} \frac{V_{in}}{L} \\ 0 \end{bmatrix} [d]$$
$$y = \begin{bmatrix} \frac{r_c R}{\left(r_c + R\right)} & \frac{R}{\left(r_c + R\right)} \end{bmatrix} \begin{bmatrix} I_L \\ V_C \end{bmatrix} \tag{11}$$

$$\begin{bmatrix} \frac{dI_L}{dt} \\ \frac{dV_C}{dt} \end{bmatrix} = \begin{bmatrix} \frac{-1}{L}\left(r_L + \frac{r_C R}{\left(r_C + R\right)} \right) & \frac{-1}{L}\frac{R}{\left(r_C + R\right)} \\ \frac{1}{c}\frac{R}{\left(r_C + R\right)} & \frac{-1}{c}\frac{1}{\left(r_C + R\right)} \end{bmatrix} \begin{bmatrix} I_L \\ V_C \end{bmatrix} + \begin{bmatrix} \frac{V_{in}}{L} \\ 0 \end{bmatrix} [d]$$
$$y = \begin{bmatrix} \frac{r_c R}{\left(r_c + R\right)} & \frac{R}{\left(r_c + R\right)} \end{bmatrix} \begin{bmatrix} I_L \\ V_C \end{bmatrix} \tag{12}$$

III. SIMULATION RESULTS

Accordingly, we compare between (10), (11) and (12) which are without parasitic elements, full model with parasitic elements and with partial parasitic elements (r_c and r_L). Hence, we present the results of open loop model according to Parameters 1 and Parameters 2 in Table 1. Figure 3 represents that the output voltages of Buck converter for *d*=0.2. Figure 4 shows that the output voltages for *d*=0.5. The transfer functions are as in (13) according to Parameters 1.

$$G_{ideal/classic} = \frac{V_O}{d} = \frac{3.507 \times 10^8}{s^2 + 152s + 2.338 \times 10^7} \left(from \text{ Eq.10} \right)$$

$$G_{(r_m = r_d = 0)} = \frac{V_O}{d} = \frac{1614\text{ s} + 3.505 \times 10^8}{s^2 + 951.8s + 2.347 \times 10^7} \left(from \text{ Eq.12} \right) \tag{13}$$

$$G_{(d=0.5)} = \frac{V_O}{d} = \frac{1614s + 3.505 \times 10^8}{s^2 + 9221s + 2.473 \times 10^7}, \quad G_{(d=0.2)} = \frac{V_O}{d} = \frac{1614s + 3.505 \times 10^8}{s^2 + 4952s + 2.408 \times 10^7} \left(from \text{ Eq.11} \right)$$

From Figure 3 and 4, as *d* decreases, the difference between linearized models and the full model with parasitic elements increases. Therefore, it can be deduced that the difference between models increases as the difference between output voltage and input voltage increases. From state space form, the pole-zero map is obtained as in Figure 5, where the poles vary significantly. Especially for Parameters 1, the poles vary significantly more.

Table 1. *Different Circuit Parameters*

	Parameters 1	Parameters 2
R	2 Ω	10 Ω
V_{nin}	15 V	24 V
L	13 μH	120 μH
c	3290 μF	330 μF
V_{D}	0.4 V	0.8 V
r_m	0.2 Ω	0.012Ω
r_c	1.4 mΩ	0.3 Ω
r_L	9 mΩ	0.08 Ω
r_D	15 mΩ	0.141Ω

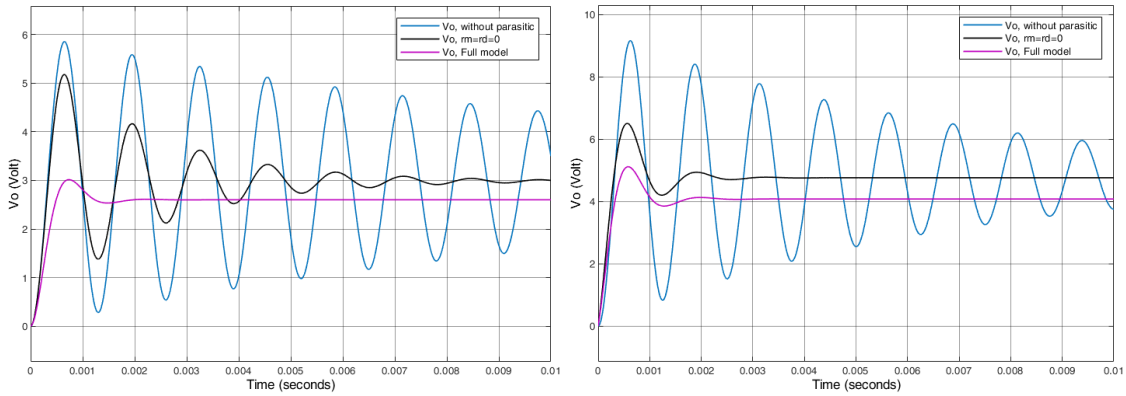

(a) ***(b)***

Figure 3. *Output voltages for d=0.2* ***(a)*** *Parameters 1 and* ***(b)*** *Parameters 2*

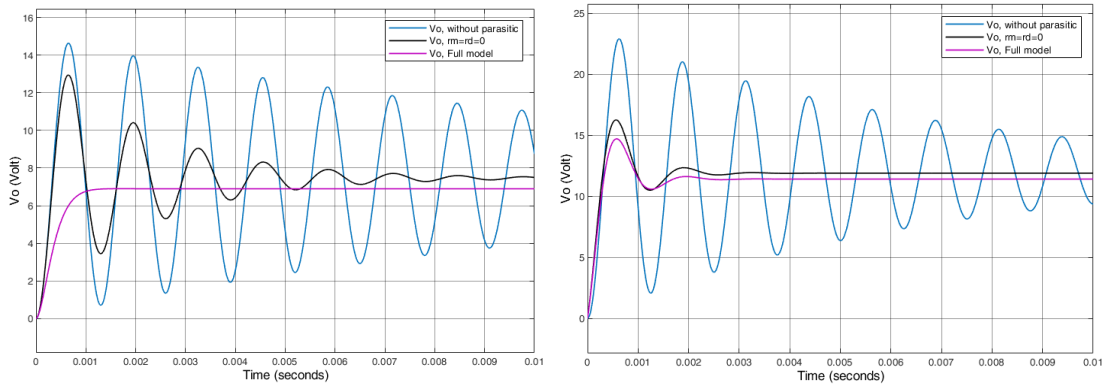

(a) ***(b)***

Figure 4. *Output voltages for d=0.5* ***(a)*** *Parameters 1 and* ***(b)*** *Parameters 2*

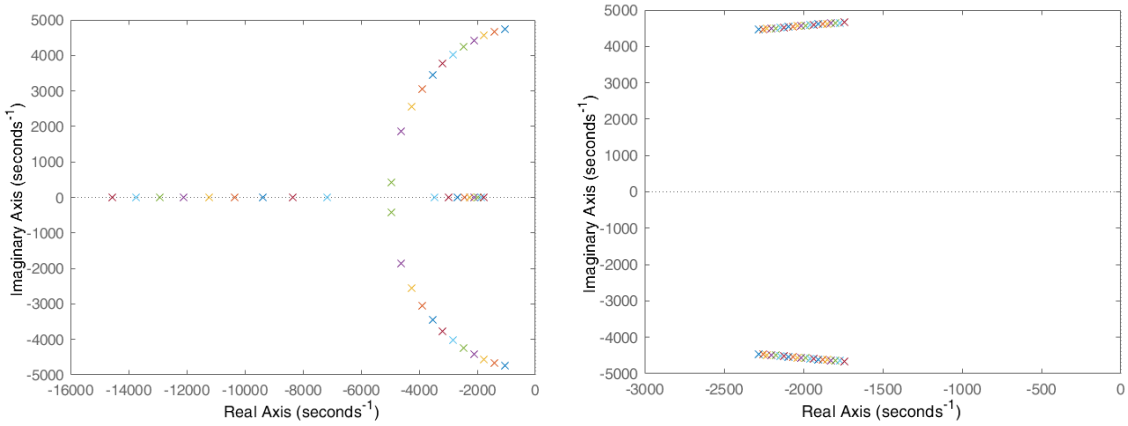

(a) ***(b)***

Figure 5. *Pole-zero map for* ***(a)*** *Parameters 1 and* ***(b)*** *Parameters 2*

Today, classic, and modern control systems are widely used in the literature. Among the classic control techniques, we can say that the PID control technique is the most widely used in industry. The reasons for this can be listed as its simplicity, low cost, not requiring high processing capacity, and easy implementation. However, this control technique is ineffective in systems that require high performance such as nonlinear systems, systems with a large parameter change range, or systems with sudden disturbances. PID control is a feedback control technique. Although PID control can yield better results, PI is not preferred in practice since the derivative effect can introduce noise. However, the derivative can be derived from integrator with filter N. The PID control system is presented in

Figure 6. The mathematical equation of the PID controller is as follows. Where *e* is the error signal, and *u* is the control input signal.

$$u(t) = K_p e(t) + K_i \int e(t) + K_D \frac{de(t)}{dt}$$

$$U(s) = \left(K_p + \frac{K_i}{s} + K_D s \right) E(s) \rightarrow U(s) = \left(K_p + \frac{K_i}{s} + K_D \frac{N}{1 + N\frac{1}{s}} \right) E(s)$$

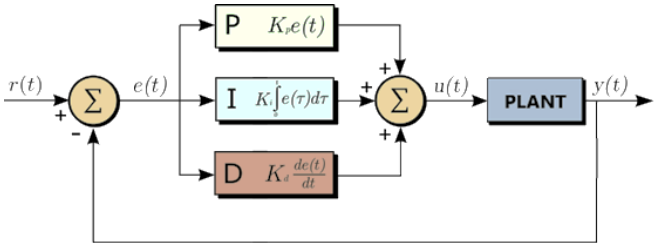

Figure 6. *PID Control block diagram*

In PI/PID control design, finding the optimum values of *P*, *I* and *D* parameters is important for control success. Different methods have been proposed in the literature for this purpose. Some of them are Ziegler-Nichols, Cohen and Coon method, Tyreus-Luyben, IMC (Internal Model Control), C-H-R (Chien, Hrones, Reswick) method, Fertik method [48], [49], [50]. Some optimization methods are also utilized [50]. Since the focus of this study is not on PID design, the PID parameters are obtained by using the "PID Tuner" tool in MATLAB Simulink. The block diagram created for this is shown in Figure 7. Clicking on the PID block opens the PID block parameters screen in Figure 7. When the "Tune" button is pressed here, the "PID Tuner" tool screen appears.
Accordingly, the parameters are arranged and adjusted according to behaviour due to input saturation after PID is designed by the tool. According to this, the PID control is designed for Parameters 1 and Parameters 2 as follows.

$$U(s) = \left(5 + \frac{700}{s} + 0.001 \frac{34926000}{1 + 34926000\frac{1}{s}} \right) E(s), \quad U(s) = \left(1 + \frac{280}{s} + 0.00018 \frac{12585586}{1 + 12585586\frac{1}{s}} \right) E(s)$$

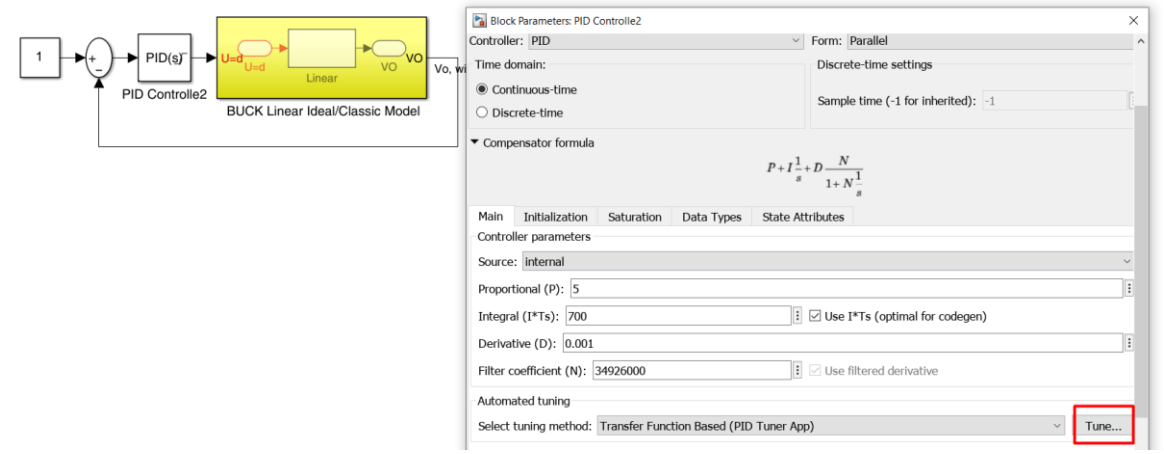

Figure 7. *"PID Tuner" Tool Screen*

Let's compare the performance of the PI controller without and with the inclusion of parasitic elements. Figure 8 shows the output voltages for a reference of 5V. The simulation results demonstrate that the designed PID control in regard to ideal/classic model in Equation (10) is successful for the

nonlinear/full model. Hence, ideal/classic model in (10) can be used for the linear controller design like PID design. However, PID is of short-time steady state error for Parameters 2.

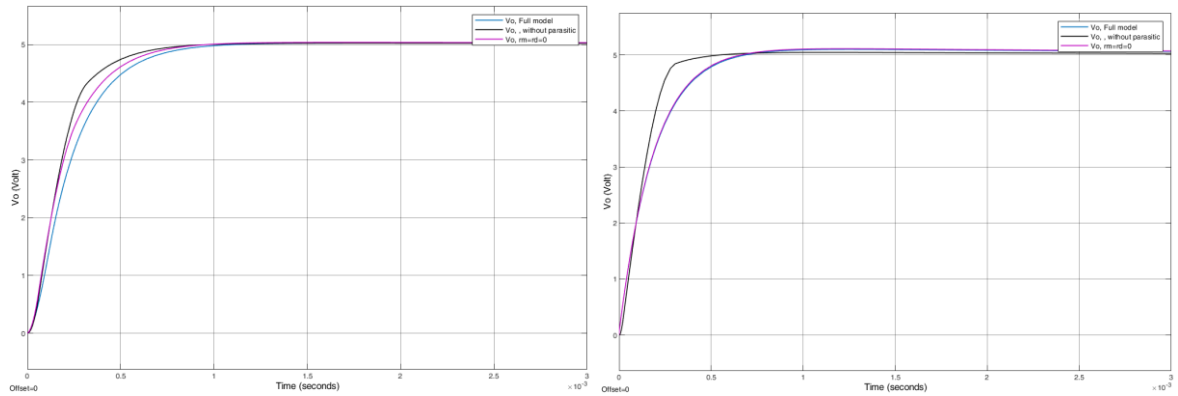

Figure 8. *The output voltages for* ***(a)*** *Parameters 1 and* ***(b)*** *Parameters 2*

We can remark on the simulation results from different perspectives as follows.

Remark 1: However, the effect of *d* in (11) should be analyzed for frequency, just as analysis is made in time domain. Therefore, bode analysis can be made to *d*. In addition, if a specific topic will not be addressed such as disturbance rejection or observer, linearized models can be utilized for PID controller design.

Remark 2: The simulation tests are conducted for only two different parameters. So, it should not be ignored that the designed PID may not be successful according to ideal/classic model in (10) when the effects of *d* in (11) are much more to the poles/zeros. This entirely depends on the values of parameters. For instance, if the input voltage of V_{in} in (11) is quite bigger than the output voltage V_O, *d* is more effective to the poles/zeros. Hence, the PID may not succeed.

Remark 3: In general, it can be interpreted that linear controller design, like PID, according to the linearized model, can be used under certain conditions. In addition, it should be applied to the full model to test its performance after PID design according to the linearized model. Moreover, the more suitable control techniques should be focused on for topics such as disturbance rejection, disturbance observer, and sensorless control.

Remark 4: The model considered in this study is valid for low and medium frequency. In this study, PWM is tried at medium frequencies such as 150-200 kHz and similar results are obtained. Since capacitance and inductance effects may also be involved at high frequencies, they need to be examined separately.

IV. CONCLUSION

This study examines the PID control design performance for a simple buck converter. For this purpose, the analysis is performed both on the effect of parasitic elements and the ideal/classical model where parasitic elements are neglected. The findings indicate that, under certain conditions, PID and similar low-order linear controllers designed according to the linearized model can be implemented to the full/non-linear model containing parasitic elements. Simulation results reveal that PID performance may be weakened in circuits where the difference between input and output voltage is large, and the values of the circuit parameters increase the effect of *d*. In general, it can be interpreted that linear controller designs such as PID based on linearized models can often be

implemented under certain conditions. However, it is imperative to verify their performance on the fully nonlinear model after PID design using the linearized model. Additionally, emphasis should be placed on investigating more appropriate control techniques to overcome challenges such as rejection of disturbances, use of disturbance observers, and implementation of sensorless control. Consequently, it can be concluded that designing PID control and similar low-order linear controllers based on linear Buck models depends on design priorities and effect of Buck converter parameters on duty cycle *d*.

V. REFERENCES

[1] S. Mukherjee, J. M. Ruiz, and P. Barbosa, "A high power density wide range DC–DC converter for universal electric vehicle charging," *IEEE Transactions on Power Electronics*, vol. 38, no. 2, pp. 1998–2012, 2023, doi: 10.1109/TPEL.2022.3217092.

[2] A. S. *et al.*, "Distinguished DC-DC converter for an electric vehicle," in *2022 6th International Conference on Computing Methodologies and Communication (ICCMC)*, 2022, pp. 578–582. doi: 10.1109/ICCMC53470.2022.9753880.

[3] C. González-Castaño, C. Restrepo, F. Flores-Bahamonde, and J. Rodriguez, "A composite DC–DC converter based on the versatile buck–boost topology for electric vehicle applications," *Sensors*, vol. 22, no. 14. 2022. doi: 10.3390/s22145409.

[4] M. Abdolahi, J. Adabi, and S. Y. M. Mousavi, "An adaptive extended kalman filter with passivity-based control for DC-DC Converter in DC microgrids supplying constant power loads," *IEEE Transactions on Industrial Electronics*, vol. 71, no. 5, pp. 4873-4882, 2023, doi: 10.1109/TIE.2023.3283686.

[5] W. Gil-González, S. Riffo, O. D. Montoya, C. Restrepo, and J. C. Hernández, "Adaptive voltage control for second-order DC–DC Converters supplying an unknown constant power load: a generalized PBC plus damping ınjection design," *IEEE Access*, vol. 11, pp. 47390–47409, 2023, doi: 10.1109/ACCESS.2023.3275083.

[6] R. M. Fuentes *et al.*, "Gain-scheduled control design applied to classical dc–dc converters in photovoltaic systems and constant power loads," *Mathematics*, vol. 10, no. 19. 2022. doi: 10.3390/math10193467.

[7] J. Hu and Z. Wang, "Sliding mode control for DC-DC converters with unknown constant power load in renewable energy systems," in *2022 7th International Conference on Power and Renewable Energy (ICPRE)*, 2022, pp. 325–330. doi: 10.1109/ICPRE55555.2022.9960700.

[8] A. Khaligh and A. Emadi, "Modified pulse adjustment technique with variable states to control dc-dc converters operating in discontinuous conduction mode and driving constant power loads," in *2006 1ST IEEE Conference on Industrial Electronics and Applications*, 2006, pp. 1–6. doi: 10.1109/ICIEA.2006.257140.

[9] N. Sarrafan, N. Horiyat, J. Zarei, R. Razavi-Far, M. Saif, and T. Dragičević, "A novel fixed-time dynamic surface DC/DC SEPIC converter controller loaded by uncertain buck-based constant power loads," *IET Power Electronics*, vol. 15, no. 16, pp. 1831–1842, Dec. 2022, doi: 10.1049/PEL2.12350.

[10] L. Palma and P. N. Enjeti, "A modular fuel cell, modular dc–dc converter concept for high performance and enhanced reliability," *IEEE Transactions on Power Electronics*, vol. 24, no. 6, pp. 1437–1443, 2009, doi: 10.1109/TPEL.2009.2012498.

[11] M. Babazadeh and H. Karimi, "A robust two-degree-of-freedom control strategy for an

islanded microgrid," *IEEE Transactions on Power Delivery*, vol. 28, no. 3, pp. 1339–1347, 2013, doi: 10.1109/TPWRD.2013.2254138.

[12] G.-J. Jeong, I.-H. Kim, and Y.-I. Son, "Application of simple adaptive control to a DC/DC boost converter with load variation," in *2009 ICCAS-SICE*, 2009, pp. 1747–1751.

[13] C. Yao, X. Ruan, W. Cao, and P. Chen, "A two-mode control scheme with ınput voltage feed-forward for the two-switch buck-boost DC–DC converter," *IEEE Transactions on Power Electronics*, vol. 29, no. 4, pp. 2037–2048, 2014, doi: 10.1109/TPEL.2013.2270014.

[14] F. Misoc, M. M. Morcos, and J. Lookadoo, "Effect of DC-DC converter topologies and operation on the electrical performance of fuel cells," *Electric Power Components and Systems*, vol. 38, no. 7, pp. 851–861, May 2010, doi: 10.1080/15325000903489777.

[15] J. Han, X. Gu, Y. Yang, and T. Tang, "Dynamic improvement with a feedforward control strategy of bidirectional dc-dc converter for battery charging and discharging," *Electronics*, vol. 9, no. 10. 2020. doi: 10.3390/electronics9101738.

[16] M. S. H. Lipu *et al.*, "Review of electric vehicle converter configurations, control schemes and optimizations: challenges and suggestions," *Electronics*, vol. 10, no. 4. 2021. doi: 10.3390/electronics10040477.

[17] S. Chakraborty, H.-N. Vu, M. M. Hasan, D.-D. Tran, M. E. Baghdadi, and O. Hegazy, "DC-DC converter topologies for electric vehicles, plug-in hybrid electric vehicles and fast charging stations: state of the art and future trends," *Energies*, vol. 12, no. 8. 2019. doi: 10.3390/en12081569.

[18] S. Mandal and D. Mishra, "Robust control of buck converter using h-infinity control algorithm," *Proceedings of 2018 IEEE Applied Signal Processing Conference, ASPCON 2018*, pp. 163–167, 2018, doi: 10.1109/ASPCON.2018.8748623.

[19] M. Srinivasan and A. Kwasinski, "Control analysis of parallel DC-DC converters in a DC microgrid with constant power loads," *International Journal of Electrical Power & Energy Systems*, vol. 122, 2020, doi: 10.1016/J.IJEPES.2020.106207.

[20] A. A. Saafan, V. Khadkikar, M. S. El Moursi, and H. H. Zeineldin, "A new multiport dc-dc converter for dc microgrid applications," *IEEE Transactions on Industry Applications*, vol. 59, no. 1, pp. 601–611, Jan. 2023, doi: 10.1109/TIA.2022.3213235.

[21] A. Benzaouia, F. Mesquine, M. Benhayoun, H. Schulte, and S. Georg, "Stabilization of a buck converter: a saturated LMI approach," *2015 4th International Conference on Systems and Control, ICSC 2015*, pp. 37–42, 2015, doi: 10.1109/ICoSC.2015.7152762.

[22] K. K. Pandey, M. Kumar, A. Kumari, and J. Kumar, "Bidirectional DC-DC buck-boost converter for battery energy storage system and PV panel" B. Das, R. Patgiri, S. Bandyopadhyay, and V. E. Balas, Eds., Singapore: Springer Singapore, vol. 206, pp. 681–693, 2021.

[23] A. A. A. Ismail and A. Elnady, "Advanced drive system for dc motor using multilevel dc/dc buck converter circuit," *IEEE Access*, vol. 7, pp. 54167–54178, 2019, doi: 10.1109/ACCESS.2019.2912315.

[24] E. Guerrero, E. Guzmán, J. Linares, A. Martínez, and G. Guerrero, "FPGA-based active disturbance rejection velocity control for a parallel DC/DC buck converter-DC motor system," *IET Power Electronics*, vol. 13, no. 2, pp. 356–367, 2020, doi: 10.1049/IET-PEL.2019.0832.

[25] M. R. Haque and M. A. Razzak, "A buck converter-based battery charging controller for electric vehicles using modified pı control system," in *2021 IEEE International IOT,*

Electronics and Mechatronics Conference (IEMTRONICS), 2021, pp. 1–4. doi: 10.1109/IEMTRONICS52119.2021.9422646.

[26] I. A. Aden, H. Kahveci, and M. E. Sahin, "Design and implementation of single-input multiple-output DC-DC buck converter for electric vehicles," *Journal of Circuits, Systems and Computers*, vol. 30, no. 13, 2021, doi: 10.1142/S0218126621502285.

[27] T. Hong, Z. Geng, K. Qi, X. Zhao, J. Ambrosio, and D. Gu, "A wide range unidirectional ısolated DC-DC converter for fuel cell electric vehicles," *IEEE Transactions on Industrial Electronics*, vol. 68, no. 7, pp. 5932–5943, 2021, doi: 10.1109/TIE.2020.2998758.

[28] R. Araria, K. Negadi, M. Boudiaf, and F. Marignetti, "Non-linear control of dc-dc converters for battery power management in electric vehicle application," *Przegląd Elektrotechniczny*, vol. 2020, no. 3, pp. 82–88, 2020.

[29] M. S. Bhaskar *et al.*, "Survey of DC-DC non-isolated topologies for unidirectional power flow in fuel cell vehicles," *IEEE Access*, vol. 8, pp. 178130–178166, 2020, doi: 10.1109/ACCESS.2020.3027041.

[30] X. Ren, Z. Tang, X. Ruan, J. Wei, and G. Hua, "Four switch buck-boost converter for telecom DC-DC power supply applications," in *2008 Twenty-Third Annual IEEE Applied Power Electronics Conference and Exposition*, 2008, pp. 1527–1530. doi: 10.1109/APEC.2008.4522927.

[31] M. Salimi, J. Soltani, and A. Zakipour, "Adaptive nonlinear control of DC-DC buck/boost converters with parasitic elements consideration," in *The 2nd International Conference on Control, Instrumentation and Automation*, 2011, pp. 304–309. doi: 10.1109/ICCIAutom.2011.6356674.

[32] M. Salimi and A. L. Eghlim, "Passivity-based control of the DC-DC buck converters in high-power applications," in *TENCON 2014 - 2014 IEEE Region 10 Conference*, 2014, pp. 1–6. doi: 10.1109/TENCON.2014.7022387.

[33] M. Csizmadia and M. Kuczmann, "Feedback linearization with integrator of DC-DC buck converter taking into account parasitic elements," in *2021 IEEE 19th International Power Electronics and Motion Control Conference (PEMC)*, 2021, pp. 97–101. doi: 10.1109/PEMC48073.2021.9432632.

[34] M. A. Qureshi, S. Musumeci, F. Torelli, A. Reatti, A. Mazza, and G. Chicco, "A novel model reference adaptive control approach investigation for power electronic converter applications," *International Journal of Electrical Power & Energy Systems*, vol. 156, p. 109722, Feb. 2024, doi: 10.1016/J.IJEPES.2023.109722.

[35] M. Walczak and L. Bychto, "Influence of parasitic resistances on the ınput resistance of buck and boost converters in maximum power point tracking (MPPT) systems," *Electronics*, vol. 10, no. 12, 2021. doi: 10.3390/electronics10121464.

[36] A. Luchetta, S. Manetti, M. C. Piccirilli, A. Reatti, and M. K. Kazimierczuk, "Effects of parasitic components on diode duty cycle and small-signal model of PWM DC-DC buck converter in DCM," *2015 IEEE 15th International Conference on Environment and Electrical Engineering (EEEIC)*, pp. 772–777, 2015.

[37] J. Wang and H. S. Chung, "Impact of parasitic elements on the spurious triggering pulse in synchronous buck converter," in *2013 IEEE Energy Conversion Congress and Exposition*, 2013, pp. 480–487. doi: 10.1109/ECCE.2013.6646740.

[38] A. Reatti, F. Corti, A. Tesi, A. Torlai, and M. K. Kazimierczuk, "Effect of parasitic

components on dynamic performance of power stages of DC-DC PWM buck and boost converters in CCM," in *2019 IEEE International Symposium on Circuits and Systems (ISCAS)*, 2019, pp. 1–5. doi: 10.1109/ISCAS.2019.8702520.

[39] S. Bhat and H. N. Nagaraja, "Effect of parasitic elements on the performance of buck-boost converter for PV systems," *International Journal of Electrical and Computer Engineering (IJECE)*, vol. 4, no. 6, pp. 831–836, 2014, doi: 10.11591/IJECE.V4I6.6855.

[40] W. Chen *et al.*, "Impact of parasitic elements on power loss in GaN-based low-voltage and high-current dc-dc buck converter," in *2018 1st Workshop on Wide Bandgap Power Devices and Applications in Asia (WiPDA Asia)*, 2018, pp. 294–298. doi: 10.1109/WiPDAAsia.2018.8734534.

[41] Y. I. Son and I. H. Kim, "Complementary PID controller to passivity-based nonlinear control of boost converters with ınductor resistance," *IEEE Transactions on Control Systems Technology*, vol. 20, no. 3, pp. 826–834, 2012, doi: 10.1109/TCST.2011.2134099.

[42] M. Salimi, J. Soltani, G. A. Markadeh, and N. R. Abjadi, "Indirect output voltage regulation of DC–DC buck/boost converter operating in continuous and discontinuous conduction modes using adaptive backstepping approach," *IET Power Electronics*, vol. 6, no. 4, pp. 732–741, 2013, doi: https://doi.org/10.1049/iet-pel.2012.0198.

[43] R. Patel and R. Chudamani, "Stability analysis of the main converter supplying a constant power load in a multi-converter system considering various parasitic elements," *Engineering Science and Technology, an International Journal*, vol. 23, no. 5, pp. 1118–1125, 2020, doi: 10.1016/j.jestch.2020.03.007.

[44] C. Olalla, R. Leyva, A. El Aroudi, P. Garcés, and I. Queinnec, "LMI robust control design for boost PWM converters," *IET Power Electronics*, vol. 3, no. 1, pp. 75–85, 2010, doi: 10.1049/iet-pel.2008.0271.

[45] F. Mumtaz, N. Zaihar Yahaya, S. Tanzim Meraj, B. Singh, R. Kannan, and O. Ibrahim, "Review on non-isolated DC-DC converters and their control techniques for renewable energy applications," *Ain Shams Engineering Journal*, vol. 12, no. 4, pp. 3747–3763, 2021, doi: 10.1016/J.ASEJ.2021.03.022.

[46] N. Bajoria, P. Sahu, R. K. Nema, and S. Nema, "Overview of different control schemes used for controlling of DC-DC converters," in *2016 International Conference on Electrical Power and Energy Systems (ICEPES)*, 2016, pp. 75–82. doi: 10.1109/ICEPES.2016.7915909.

[47] D. Bhattacharyya, S. Padhee, and K. C. Pati, "Modeling of DC–DC converter using exact feedback linearization method: a discussion," *IETE Journal of Research*, vol. 65, no. 6, pp. 843–854, 2019, doi: 10.1080/03772063.2018.1454345.

[48] S. Anusha, G. Karpagam, and E. Bhuvaneswarri, "Comparison of tuning methods of PID controller," *International Journal of Management, Information Technology and Engineering*, vol. 2, no. 8, pp. 1–8, 2014.

[49] M. Shahrokhi and A. Zomorrodi, "Comparison of PID controller tuning methods," *Department of Chemical & Petroleum Engineering Sharif University of Technology*, pp. 1–2, 2013.

[50] F. Alhayanı, A. S. Jaber, Ç. Aydın, And D. Ç. Atilla, "Tuning of PI controller for four-area load frequency control using elephant herding optimization," *AURUM Journal of Engineering Systems and Architecture*, vol. 3, no. 2, pp. 215–225, 2019.